Barium Boron Silicate glass–ceramic for use as sealant in planar SOFC

1,[a]M.J. Silva, 2,[b]S.T.Reis, 1,[c]S.R.H. Mello Castanho

[1] Energy and Nuclear Research Institute IPEN-CNEN/USP
Av. Prof. Lineu Prestes 2242 - CEP: 05508-000 - São Paulo - Brazil
[2] Missouri University of Science and Technology
Rolla, MO 65409-1170, USA

[a]maviael.jose@usp.br , [b]Signo.T.Reis@saint-gobain.com
[c]srhmelo@ipen.br

ABSTRACT

Glass-ceramic seals play an important role in the performance of the solid oxide fuel cell (SOFC). In this work glass-ceramic seals are discussed from the point of view of the thermal behavior of the glass and the electrochemical parameters obtained from polarization curves such as corrosion current densities (i_{corr}), and corrosion potential (E_{corr}). A seal material must have a combination of thermal-mechanical and electrochemical properties in order to seal cell components and stacks and prevent side reactions. It must be stable in oxidizing and reducing atmospheres and withstand thermal cycles between room temperature and the cell operating temperature (800 to 900°C). Glass-ceramics in the system BaO–B_2O_3–Al_2O_3–SiO_2 were investigated and compared from the point of view of sealing ability. Dilatometric analysis, thermal stability against crystallization, microstructure and electrochemical durability are discussed.

KEY- WORDS: Solid Oxide Fuel Cells, sealants, glass-ceramic

1. Introduction

In planar SOFC, fuel gas and air must kept apart from each other to avoid three main critical situations. Firstly damages in terms of efficiency to produce energy, secondly avoid aside reactions among cell components and last but not least local overheating[1,2,3]. The sealants for SOFC's must meet the following demands: should have a CET that matches in an acceptable level that of the other fuel cells components, must exhibit no adverse reactions with

the joining components, and the sealant must have high chemical stability in reducing and oxidizing atmospheres[3]. It is well known that the chemical composition plays an important role in the corrosion behavior of glasses [3].However, how the amorphous structure affects the corrosion behavior of glasses is a long-term puzzling problem. It is recognized that unlike crystal alloys, glasses present unique structural characteristics without long-range periodic lattice. This structural variation in atom scale could theoretically induce even larger changes in their electrochemical properties. Nevertheless many studies have been directed only toward thermal properties in detrimental of the electrochemical properties[3,5].

Therefore in order to develop a suitable glass-ceramic sealant, it is necessary to understand the chemical interaction and corrosion behavior of the sealant under severe service environment (both oxidizing and reducing). This work provides an understanding of this interactions and presents the thermal and corrosion behavior of the studied sealants.

2. Experimental

The infrared spectra of the glasses were recorded at room temperature using the KBr disc technique. A Thermo Nicolet Nexus 870 FTIR spectrometer was used to obtain the spectra in the wave number range between 400 and 2000 cm-1 with a resolution of 2 cm^{-1}. Characteristic temperatures (glass transition temperature Tg, onset and maximum crystallization temperature Tx1 and Tx2, melting temperature Tm) were determined by differential scanning calorimetry (DSC) using a SETARAM MHTC 96 calorimeter at a heating rate of 10 ºC/min. The Coefficient of Thermal Expansion (CTE) of the glasses was measured using a LINSEIS L75VD1750C dilatometer with a heating rate of 5 ºC/ min. The samples were analyzed by X-ray diffraction (XRD) with monochromatic CuKα radiation (λ = 0.1542 nm) using a RIGAKU DMAX 2000 PC equipment.

All electrochemical measurements were conducted using a AUTOLAB PGSTAT 30 Electrochemical Measurement System. Potentiodynamic polarisation curves were measured with a potential sweep rate of 50 mVref /s in 3.0 M NaOH and HCL 2.0 M aqueous solution after immersing the samples for about 30 min, when the open-circuit potential reached a steady state. All the potentials mentioned in this work were all referred to Ag/AgCl (saturated). Each electrochemical measurement was tested at least three times for repeatability. Only typical curves from an average of all measurements are presented results. All the samples were chacacterized by scaning electron microscopy SEM (Hitachi TM 3000) after polishment. Chemical compositions of the glass are listed in Table 1. Reagent grade BaOH, H_3BO_3, SiO_2 and Al_2O_3 > 99 wt% purity were chosen as the starting materials. After mixing the batches were melted at 1500º C for 1,5 h. The molten glass was annealed at 650º C for 1 h before cooling down to ambient temperature. The bulk glass were milled into powder (45-50µm) for the IR, DSC, and CTE tests. The barium aluminosilicate system(BAS, $BaO–Al_2O_3–SiO_2$) was chosen as the starting point for glass composition development because of its potential for good glass-forming properties. The Chemical compositions of the glasses are listed in Table 1.

Table 1 Batch compositions

Glass ID	Chemical Composition (wt %)			
	BaO	B_2O_3	SiO_2	Al_2O_3
BAS-2	77	7	11.5	4.5
BAS-4	74	4	19	3

2. Results and discussion

Figure 1 shows the infrared absorption spectra of the $BaO– Al_2O_3–B_2O3–SiO_2$ glassy samples BAS-2 and BAS-4. The band at about 471 cm^{-1} is due to Si–O–Si asymmetric bending vibration and the small shoulder located at 724 cm^{-1} is attributed to bending vibration of B–O–B in [BO_3] triangles [4]. The main intense band located at 850–1100 cm^{-1} represents a superposition of two bands

situated close to each other at about 925 and 1012 cm^{-1}, the absorption peak near 925 cm-1 is assigned to the stretching vibration of [BO_4] tetrahedral and the band near 1012 cm^{-1} is due to the combined stretching vibrations of Si–O–Si and B–O–B network of tetrahedral structural units [7,8]. The shoulder at 1320 cm^{-1} is due to the stretching vibration of the boroxol ring and the band centered at 1140 cm^{-1} is attributed to the B–O stretching vibration of [BO_3] triangles, characteristic for the [BO_3] group [4,5].

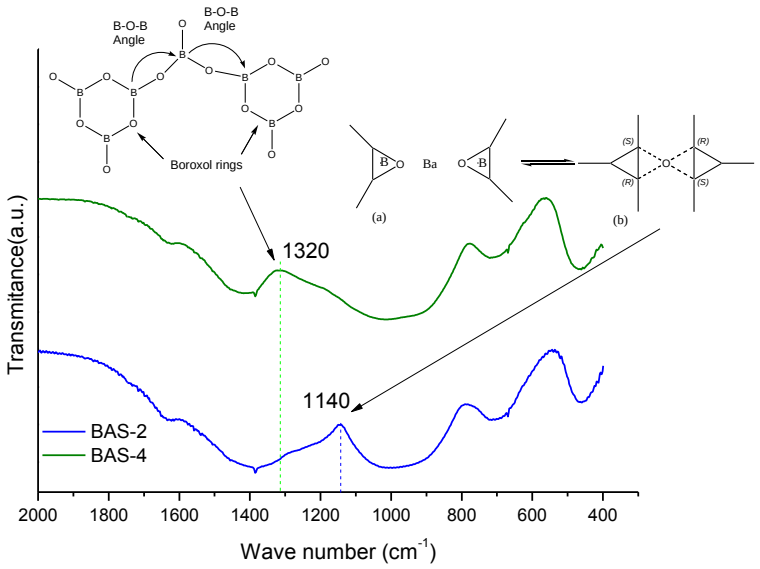

Figure 1 FT-IR spectra of the glass BAS-2 and BAS-4

Figure 2 shows the DSC curves of glass samples. Glasses BAS-2 and BAS-4 show two exothermic peaks, the exothermic peak of BAS-2 being very weak. The characteristic temperatures and glass stability parameters are listed in Table 2. It can be seen that an increase of Al_2O_3 (5 % wt) leads to a decrease of T_g and an increase of ΔTx. This suggests that the introduction of Al_2O_3 to the glass system helps to improve glass stability and to decrease the trend to crystallization. A parameter usually employed to estimate the glass stability is the thermal stability, which is defined by $\Delta T_x = T_x - T_g$ [3,5,8], an increasing $\Delta T_x = T_x - T_g$indicate an increasing glass stability and a lower tendency toward crystallization.

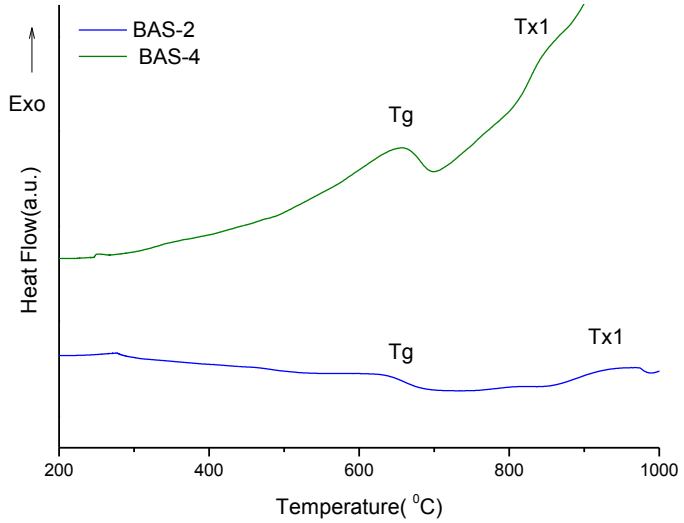

Figure 2 DSC curves of glass samples BAS-2 and BAS-4

The values of thermal expansion coefficient are calculated for each sample using dilatometric analysis. The plots obtained by dilatometer are shown in Fig. 3 for samples BAS-2, and BAS-4 respectively. Basically, thermal expansion depends on the bond strength. The values obtained from the plot TEC are given in Table 2.

Table 2 Summary of the thermal properties of glasses

Glass ID	Tg(ºC)	Tx	Tx2	Tm1	Tm2	ΔTx	CET(20 to 700ºC)x10^6 °C
BAS-2	488	593	766	992	-	105	5.4
BAS-4	630	819	916	-	-	189	9.7

Glass that best fulfills the cell requirement such as thermal expansion coefficient should lie in the range 8.5 to 12 ppm/ºC [10,11]. The value of TEC obtained for the glass sample BAS-4 is very near to this specified range therefore it's suitable for SOFC sealant application.

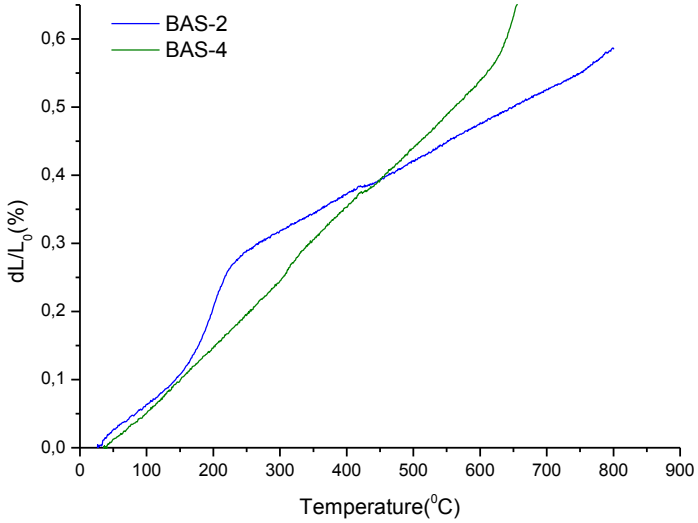

Figura 3 Plot of Dilatometer of BAS-2 and BAS-4 samples

Fig. 4 presents the XRD patterns of the as-prepared BAS- glasses. The appearance of a broad halo at the angle of 2Θ ≈ 30º and the absence of any diffraction peaks associated with crystalline phases indicate that the amorphous structure was formed in the annealed glasses.

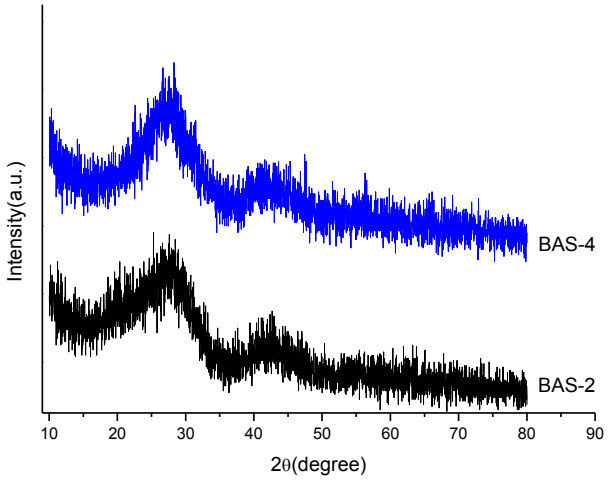

Figure 4 X-ray diffraction patterns of BAS-2 and BAS-4 glass powder

As shown in Figure 5 the scanning electron microscopy(SEM) demonstrates droplet-shaped immiscibility regions evolved in a homogeneous matrix as a result of a simple primary process[10,11].

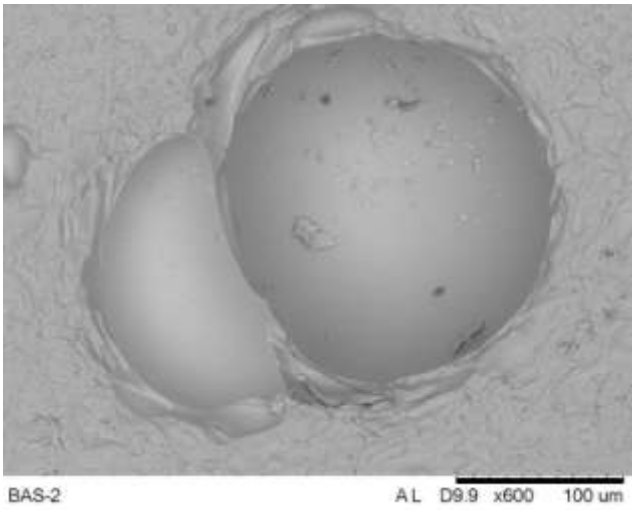

Figure 5 SEM image of the sample BAS-2

Figure 6 represented a SEM picture of the BAS-4 sample, the process of phase separation lead to the formation of halos around microphase droplets. Halos, in this case SiO_2 , around droplet-shaped strongly affects the chemical properties of a glass[11].

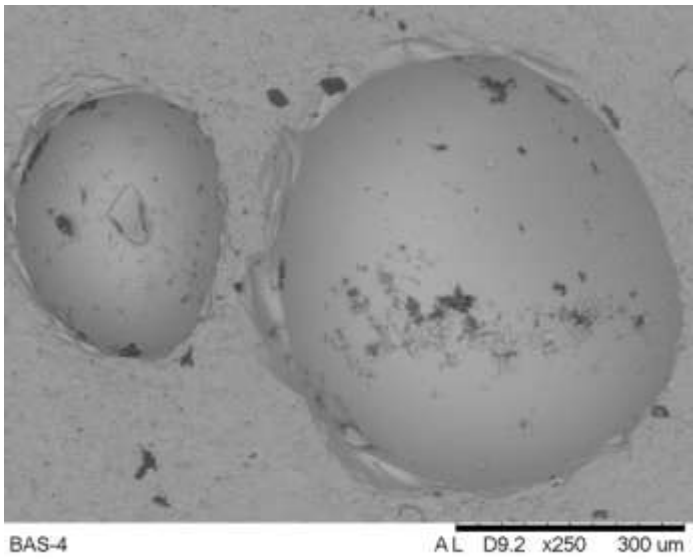

Figure 6 SEM image of the sample BAS-4

Some important electrochemical parameters (including anodic and cathodic Tafel slopes, βa and βc) attained from the potentiodynamic polarization curves are summarized in Table 3.

Table 3 Sumary of the electrochemical parameters of each sample obtained from potentiodynamic polarization curves

Sample	$E_{corr}(mV_{ref})$	$I_{corr}(A/cm^2)$	β_a (V_{ref})/dec	β_c (V_{ref}/dec)
BAS-2	-339	$6,67x10^{-7}$	3,235	2,533
BAS-4	-550	$7,701x10^{-6}$	2,308	1,88

Fig. 7 shows the potentiodynamic polarisation curves for the BAS-2 and BAS-4 samples in 3.0 M NaOH aqueous solution. The corrosion current densities (icorr) were derived using Tafel extrapolation method by linear fitting of strong polarised zone (i.e. the potential is above ±100 mVref from the open-circuit potential) [9]. The corrosion current densities calculated from Tafel extrapolation method are in the order of 10^{-7} A/cm^2. All samples are passivated spontaneously with a passive current density in the order of 10^{-6} A/cm^2.

As can be seen from the polarisation curves, there is slights differences in the polarization behaviour for the BAS-4 and its counterpart, the sample BAS-2. However, the sample BAS-4 exhibits the most negative corrosion potential (Ecorr), and the maximum corrosion current density. Consequently, the BAS-4 sample holds the highest dissolution trend and the lowest corrosion resistance compared with the BAS-2 sample, which is in according with SEM observation.

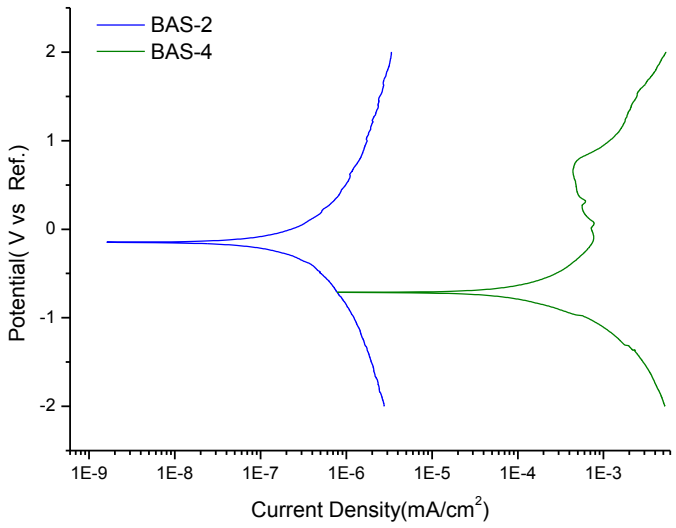

Figure 7 Potentiodynamic polarisation curves of the glasses, BAS-2 and BAS-4 measured with a potential sweep rate of 50m V_{ref}/s in 3.0 M NaOH aqueous solution

The cathodic shift observed for the BAS-4 sample with 19 %(wt) of SiO_2 indicates that the incorporation of silica alters the cathodic kinetics on the sample surface. It is also observed that the polarization curves of the sample BAS-4 have regions of activation /passivation behavior due probably to the formation of a thin layer composed by Al_2O_3 . Consequently, the sample BAS-4 holds the highest dissolution trend and the lowest corrosion resistance compared with the sample BAS-2, which is in according with SEM observation[5,7,9].

3.Conclusion

Two glasses were prepared based on the $BaO–Al_2O_3–SiO_2$ system with the addition of B_2O_3 by the melting–annealing method in an effort to develop a suitable sealant for planar SOFC. The chemical composition play an important role in the corrosion behavior of glasses. The glass labeled BAS-4 matches the desired thermo-physical properties for SOFC seals.

The authors would like to thank the Missouri University of Science and Technology at Rolla. This work was supported by the Energy and Nuclear Research Institute IPEN-CNEN, and the University of São Paulo USP.

References

[1] WRIGHT, E.i.; RAHIMIFARD, S.; CLEGG, A.j. Impacts of environmental product legislation on solid oxide fuel cells. **Journal of Power Sources**. v. 190, n. 2, p.362-371. 15 may 2009.

[2] THEERAPAPVISETPONG, A.; JIEMSIRILERS, S.; THAVORNITI, P.; CONRADT, R. Barium-Free Glass-Ceramic Sealants from the System $CaO-MgO-B_2O_3-Al_2O_3-SiO_2$ for Application in the SOFC. **Materials Science Forum**, v. 695, p. 1-4, 2011

[3] FERGUS, J. W. Sealants for solid oxide fuel cells. **Journal of Power Sources**, v. 147, n.1-2,p.46-57, 2005.

[4] ELBATAL, F. H. .; KHALIL, M. M. .; NADA, N.; DESOUKY, S. . Gamma rays interaction with ternary silicate glasses containing mixed CoO+NiO. **Materials Chemistry and Physics**, v. 82, n. 2, p. 375-387, 2003.

[5] MAHAPATRA, M. K.; LU, K. Seal glass for solid oxide fuel cells. **Journal of Power Sources**, v. 195, n. 21, p. 7129-7139, 2010.

[6] LIN, S. E.; CHENG, Y. R.; WEI, W. C. J. BaO–B2O3–SiO2–Al2O3 sealing glass for intermediate temperature solid oxide fuel cell. **Journal of Non-Crystalline Solids**, v. 358, n. 2, p. 174-181, 2012.

[7] LAORODPHAN, N.; NAMWONG, P.; THIEMSORN, W. et al. A low silica, barium borate glass–ceramic for use as seals in planar SOFCs. **Journal of Non-Crystalline Solids**, v. 355, n. 1, p. 38-44, 2009

[8] REIS, S. T.; PASCUAL, M. J.; BROW, R. K.; RAY, C. S.; ZHANG, T. Crystallization and processing of SOFC sealing glasses. **Journal of Non-Crystalline Solids**, v. 356, n. 52-54, p. 3009-3012, 2010.

[9] VANOOIJ, W.; ZHU, D.; STACY, M. et al. Corrosion Protection Properties of functional Silanes—An Overview. **Tsinghua Science & Technology**, v. 10, n. 6, p. 639-664, 2005.

[10] CHOU, Y.-SHYUNG; THOMSEN, E. C.; CHOI, J.; STEVENSON, J. W. Compliant alkali silicate sealing glass for solid oxide fuel cell applications : Combined stability in isothermal ageing and thermal cycling with YSZ coated ferritic stainless steels. **Journal of Power Sources**, v. 197, p. 154-160, 2012.

[11] WEGNER, S.; VAN WÜLLEN, L.; TRICOT, G. The structure of phosphate and borosilicate glasses and their structural evolution at high temperatures as studied with solid state NMR spectroscopy: Phase separation, crystallisation and dynamic species exchange. **Solid State Sciences**, v. 12, n. 4, p. 428-439, 2010.